

CHAPTER 3

Fission products yield in the neutron-induced fission of ^{232}Th with average energies of 5.42 MeV, 7.75 MeV and 10.09 MeV

3.1 Introduction	44
3.2 Preparation of Lithium Target by Rolling Technique	45
3.3 Experimental method	47
3.4 Analysis of Experimental Data	49
3.4.1 Calculation of the neutron energy	49
3.4.2 Calculation of the fission yields	50
3.5 Results and Discussions	50
3.6 Summary and Conclusions	57
References	58

Published in:

1. **P.M. Prajapati** *et al.*, Fission products yields in the neutron-induced fission of ^{232}Th with average energies of 5.42 MeV, 7.75 MeV and 10.09 MeV, *Nuclear Science and Engineering*, 2012 (*communicated*)

3.1 Introduction

The development of ADS [1-4] systems and advanced reactor programme requires significant amount of new and improved nuclear data [5] in extended energy regions as well as for a variety of new materials. Accurate nuclear data such as fission yields, neutron capture cross-sections, fission cross-sections and decay data including half-lives, decay energies, branching ratio, etc. are required for many advanced reactor calculations. Further, the advent and development of advanced reactors have highlighted the need for accurate determination of fission yields in the fission of actinides induced by neutrons.

In any nuclear reactor, the neutron spectrum has the continuous energy ranging from 0 to 15 MeV which depends upon the particular reactor design whereas in ADS the energy of neutron goes up to 200 MeV. This is because in ADS high energy (GeV) protons from an accelerator strike a heavy elements target like Pb and Bi yields a large number of high-energy neutrons by spallation reaction. Thus, ^{232}Th - ^{233}U fuel in connection with ADS has to face neutron energies of wide range. The high energy neutrons can cause fission of ^{232}Th besides activation to produce ^{233}U at lower energy. Thus, it is important to measure the yields of the fission products in the high energy neutron induced fission of ^{232}Th . The yields of short-lived fission products and independent yields of various fission products are important for decay heat calculation. Further, the yields of fission products are also needed for mass and charge distribution studies, which can provide valuable information for understanding the nuclear fission process.

A literature survey [6-16] indicates that sufficient data in the reactor neutron [6-8] and mono-energetic [9-13] neutron-induced fission of ^{232}Th are available in a wide energy ranging from 1 MeV to 14.8 MeV. From these data, it is found that the fission yields for reactor neutron, 3 MeV [9] to 14.8 MeV [10-13] mono-energetic neutron-induced fission of ^{232}Th are available in exhaustive way. However, for other mono-energetic neutron induced fission of ^{232}Th are available from the work of Trochon et al [14], Glendenin et al [15] and Lam et al [16]. From these data, it can be seen that peak to valley (P/V) ratio decreases from neutron energy of 1 MeV to 14.8 MeV. Further, it can also be seen that the fine structure around the mass number 134 - 135, 139 - 140, 144 - 145 and their complementary products decreases with increase of neutron energy. In order to examine the latter aspect, the yields of various fission products in the neutron-induced fission of ^{232}Th have been determined using recoil catcher and off-line gamma-ray

spectrometric technique with average energies of 5.42 MeV, 7.75 MeV and 10.09 MeV. The present measured fission yield data have been compared with similar data from mono-energetic neutron induced fission of ^{232}Th to examine the nuclear structure effect.

3.2 Preparation of Lithium Target by Rolling Technique

The Lithium target has been prepared by Rolling Technique at target laboratory of Bhabha Atomic Research Centre-Tata Institute of Fundamental Research (BARC-TIFR) Pelletron Facility, Mumbai. Stainless steel plates were generally used to roll the metals but Li sticks to the stainless steel pack while rolling. Therefore, Li has been prepared by using stainless steel plates and inserting a very small amount of silicon oil between the lithium metal and the stainless steel plates. But sometimes the pin holes were observed in the foils. Hence, Teflon plates have been used for rolling. A small Li lump kept in paraffin oil or kerosene is cut and made it flat by cutting with a knife. Then, it was wiped with tissue paper carefully. It was then placed between 2 Teflon plates of dimension 50 mm x 50 mm x 0.7/0.8mm and rolled one way for 2-3 times and again 2-3 times by changing the direction of Li. It was then removed and cut into a rectangular shape. This rectangular shape Li foil was weighed and its area was measured and thickness was calculated. The procedure was repeated till the required thickness was achieved. Minimum pressure was applied for each rolling. The rolling mill used for the Li sample preparation is given in Fig.3.1.

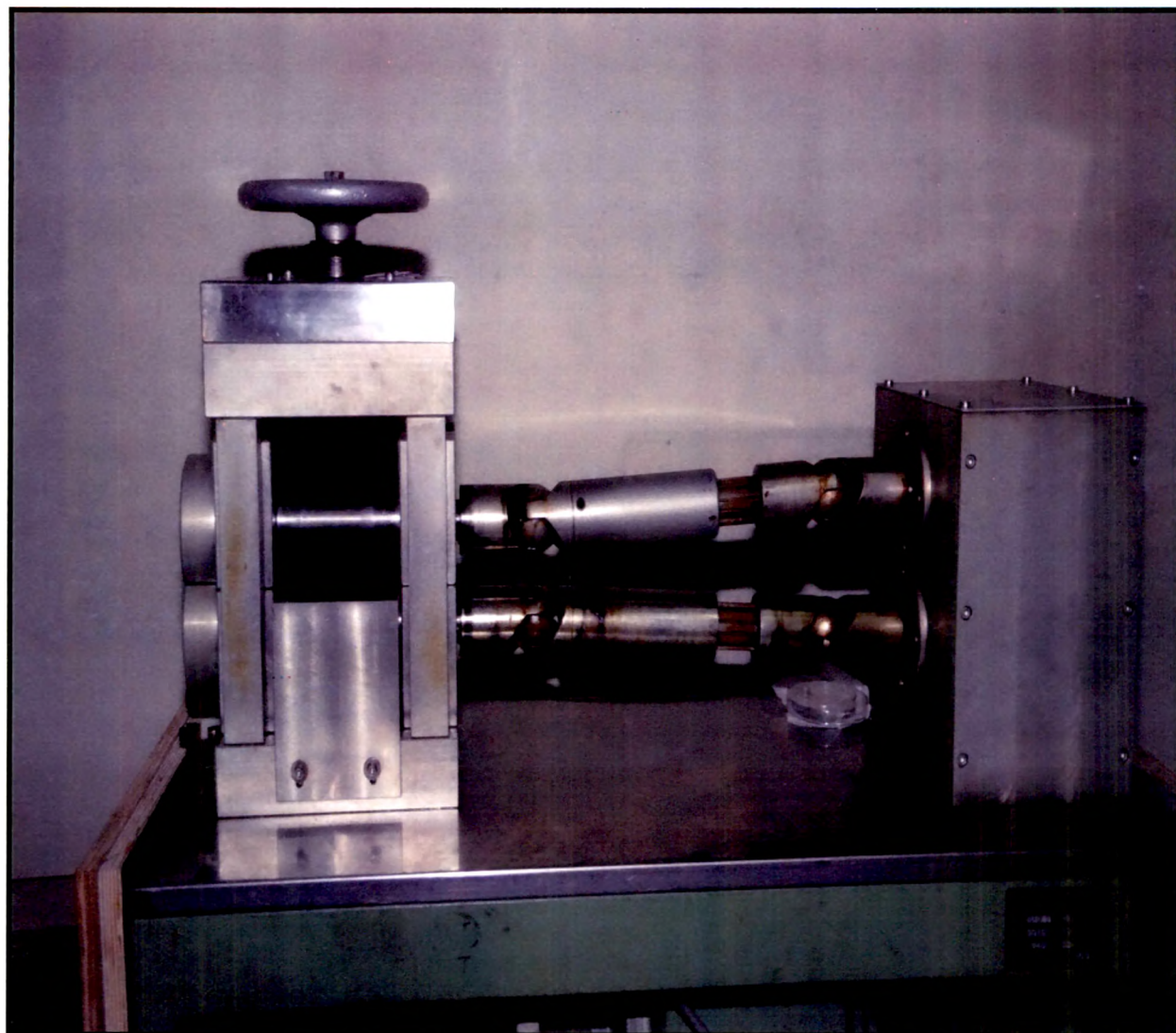


Fig. 3.1 The rolling mill at target laboratory, BARC-TIFR Pelletron Facility, Mumbai

3.3 Experimental method

The experiment was carried out using the 14 UD BARC-TIFR Pelletron Facility at Mumbai, India. A schematic diagram of BARC-TIFR Pelletron facility is given in Fig. 3.2. The neutron beam was obtained from the ${}^7\text{Li}(p,n)$ reaction [17] by using the proton beam main line at 6 m above the analyzing magnet of the Pelletron facility to utilize the maximum proton current from the accelerator. The energy spread for proton at 6 m was maximum 50-90 keV. At this port, the terminal voltage was regulated by GVM mode using terminal potential stabilizer. Further, we used a collimator of 6 mm diameter before the target. The lithium foil was made up of natural lithium with thickness 3.7 mg/cm^2 , sandwiched between two tantalum foils of different thickness. The front tantalum foil facing the proton beam was the thinnest one, with thickness of 3.9 mg/cm^2 , in which degradation of proton energy was only 30 keV [18]. On the other hand, the back tantalum foil was the thickest (0.025 mm), which was sufficient to stop the proton beam. Behind the Ta-Li-Ta stack, the sample used for irradiation was natural ${}^{232}\text{Th}$ metal foil, which was wrapped with 0.025 mm thick aluminum foil. The aluminum wrapper was used to stop and collect the fission products recoiling out from the surface. The size of ${}^{232}\text{Th}$ metal foil was 1.0 cm^2 with thickness of 29.3 mg/cm^2 . The ${}^{232}\text{Th}$ metal foil wrapped with aluminum was mounted at zero degree with respect to the beam direction at a distance of 2.1 cm from the location of the Ta-Li-Ta stack. Different sets of samples were made for each irradiation at various neutron energies.

The Ta-Li-Ta and ${}^{232}\text{Th}$ meta foil were irradiated at proton energies (E_p) of 7.8 MeV, 12 MeV and 18 MeV for a period of 15 h, 6 h and 5 h, respectively depending upon the energy of proton beam facing the tantalum target. The proton current during the irradiations varied from 100 nA to 400 nA. After irradiation, the samples were cooled for one hour. Then the irradiated target of Th along with Al wrapper were mounted on Perspex plate and taken for γ -ray spectrometry. The γ -rays of fission/reaction products from the irradiated Th sample were counted in energy and efficiency calibrated 80 c.c. HPGe detector coupled to a PC-based 4K channel analyzer. The counting dead time was kept always less than 5 % by placing the irradiated Th sample at a suitable distance from the detector to avoid pileup effects.

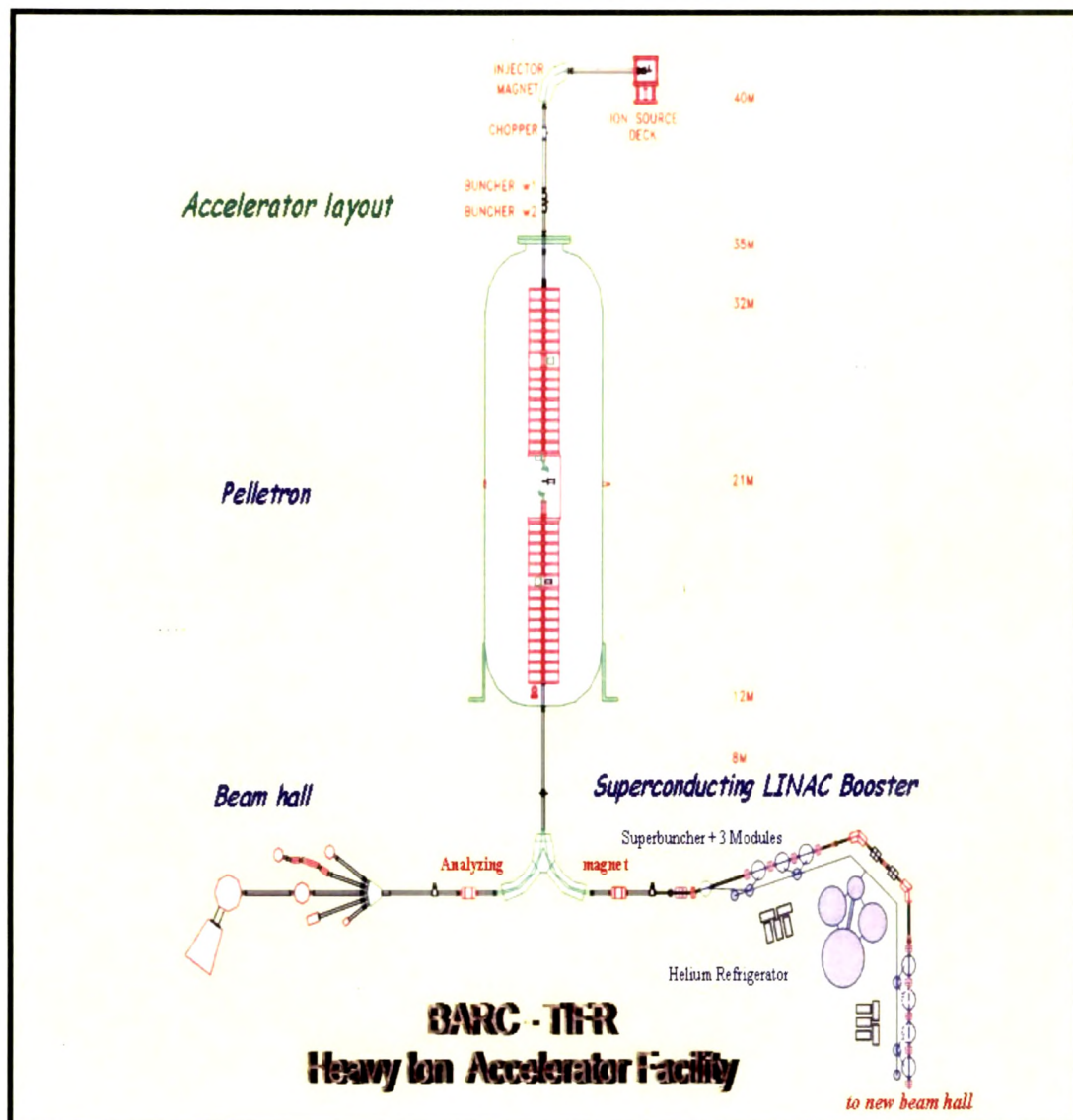


Fig. 3.2 A schematic diagram BARC-TIFR Pelletron Facility, Mumbai

The energy and efficiency calibration of the detector system was done by counting the γ -ray energies of standard ^{152}Eu source keeping the same geometry, where the summation error was negligible. This was checked by comparing the efficiency obtained from γ -ray counting of standards such as ^{241}Am (59.54 keV), ^{133}Ba (80.997, 276.4, 302.9, 356.02 & 383.82 keV), ^{137}Cs (661.66 keV), ^{54}Mn (834.55 keV), ^{60}Co (1173.23 & 1332.5 keV). The detector efficiency was 20 % at 1332.5 keV relative to 3" diameter x 3" length NaI(Tl) detector. The uncertainty in the efficiency was 2-3 %. The resolution of the detector system had a FWHM of 1.8 keV at 1332.5 keV of ^{60}Co . The γ -ray counting of the irradiated Th sample was done up to few months to check the half-life of the nuclides of interest.

3.4 Analysis of Experimental Data

3.4.1 Calculation of the neutron energy

In the present experiment, the incident proton energies were 7.8 MeV, 12 MeV and 18.0 MeV. The degradation of the proton energy in the front thin tantalum foil was only 50-80 keV. The Q-value for the $^7\text{Li}(p, n)^7\text{Be}$ reaction to the ground state is -1.644 MeV whereas the first excited state is at 0.431 MeV above the ground state leading to the Q-value -2.079 MeV. Therefore, for the proton energies of 7.8 MeV, 12 MeV and 18.0 MeV, the resulting peak energy for the first group of neutrons (n_0) is 5.92 MeV, 10.12 MeV and 16.12 MeV. The corresponding neutron energy of the second group neutrons (n_1), for the first excited state of ^7Be are 5.42 MeV, 9.63 MeV and 15.62 MeV for the proton energies of 7.8 MeV, 12 MeV and 18.0 MeV, respectively. C. H. Poppe et al [19] have given the branching ratio to the ground state and first excited state of ^7Be for $E_p = 4.2$ MeV to 26 MeV. Further, the fragmentation of ^8Be to $^4\text{He} + ^3\text{He} + n$ ($Q = -3.23$ MeV) occurs and other reaction channel opens to give a continuous neutron energy distribution besides n_0 and n_1 groups of neutrons above $E_p = 4.5$ MeV. To observe the trend of a continuous neutron spectrum besides from n_0 and n_1 groups of neutrons for the proton energies of 7.8 MeV, 12 MeV and 18.0 MeV, the neutron spectrum have been generated [20, 21] using the neutron energy distribution given by C. H. Poppe et al. The figures of neutron spectrum have been given in chapter 4. Based on the neutron spectrum, the flux weighted average neutron energy has been calculated as 5.42 MeV, 7.75 MeV and 10.09 MeV for the proton energies of 7.8 MeV, 12 MeV and 18 MeV, respectively.

3.4.2 Calculation of the fission yields

The photo-peak areas of different γ -rays of interest were calculated by subtracting the linear background from their net peak areas. The number of γ -rays detected (A_{obs}) under the photo-peak of each individual fission products is related to the cumulative yield (Y_c) with the following relation,

$$A_{\text{obs}} (\text{CL/LT}) = N\sigma_f(E)\phi I_\gamma \varepsilon Y_c (1 - e^{-\lambda t}) e^{-\lambda T_c} (1 - e^{-\lambda LT}) / \lambda \quad (1)$$

where,

N = number of target atoms,

$\sigma_f(E)$ = neutron-induced fission cross-section as a function of neutron energy (E) of the target with average neutron flux (ϕ)

I_γ = branching intensity for the γ -ray of the fission product

ε = efficiency

t = irradiation time, T_c = cooling time

CL and LT = clock time and live time of counting respectively

The nuclear spectroscopic data such as the γ -ray energy, branching intensity and half-life of the fission products are taken from ref. [22]. The cumulative yields of the fission product relative to fission rate monitor ^{92}Sr were calculated using eq. (1). The yield of fission rate monitor ^{92}Sr was chosen from the point of view of the near constant yield with change of neutron energy [15]. For neutron energies of 5.42 MeV, 7.75 MeV and 10.09 MeV, the fission yield data of ^{92}Sr in the neutron induced fission of ^{232}Th with neutron energy of 5.9 MeV, 7.6 MeV and 8.0 MeV was taken from ref. [15].

3.5 Results and Discussions

The cumulative yields of various fission products relative to ^{92}Sr in the neutron-induced fission of ^{232}Th at flux weighted average neutron energies of 5.42 MeV, 7.75 MeV and 10.09 along with nuclear spectroscopic data are given in Tables 3.1, 3.2 and 3.3 respectively.



Table 3.1 Fission product yields in neutron-induced fission of ^{232}Th with average energy of 5.42 MeV

Nuclide	Half-life	Gamma-ray energy (keV)	Gamma Abundance (%)	Fission yield (%)	
				Present Data	Literature [15]
^{91}Sr	9.63 h	749.8	23.3	5.37 ± 0.59	6.63 ± 0.21
^{92}Sr	2.71 h	1384.9	90.0	6.56 ± 0.78	6.56 ± 0.81
^{97}Zr	16.74 h	743.3	93.03	5.01 ± 0.30	4.80 ± 0.13
^{99}Mo	65.97 h	140.5	89.4	3.49 ± 0.12	3.79 ± 0.23
^{132}Te	3.204 d	228.1	88.0	4.01 ± 0.48	3.80 ± 0.13
^{133}I	20.8 h	529.9	87.0	3.65 ± 0.25	5.64 ± 0.19
^{135}I	6.57 h	1131.5	22.6	6.16 ± 0.23	5.98 ± 0.19
		1260.4	28.7	5.77 ± 0.32	

Table 3.2 Fission product yields in neutron-induced fission of ^{232}Th with average energy of 7.75 MeV

Nuclide	Half-life	Gamma-ray energy (keV)	Gamma Abundance (%)	Fission yield (%)	
				Present Data	Literature[15]
$^{85}\text{Kr}^{\text{m}}$	4.48 h	151.1	75.0	4.59 ± 0.27	6.01 ± 0.26
^{87}Kr	76.3 m	402.5	50.0	5.35 ± 0.32	7.10 ± 0.35
^{88}Kr	2.84 h	196.3	26.0	5.77 ± 0.46	7.03 ± 0.30
$^{91}\text{Y}^{\text{m}}$	49.71 m	555.5	95.0	5.45 ± 0.35	
^{91}Sr	9.63 h	749.8	23.3	6.54 ± 0.58	7.15 ± 0.21
		1024.0	33.0	6.50 ± 0.71	
^{92}Sr	2.71 h	1384.9	90.0	6.45 ± 0.53	6.45 ± 0.78
^{97}Zr	16.9 h	743.3	93.03	2.51 ± 0.12	3.62 ± 0.13
^{99}Mo	65.97 h	140.5	89.4	2.38 ± 0.35	2.21 ± 0.13
^{132}Te	3.204 d	228.1	88.0	3.09 ± 0.18	2.78 ± 0.11
^{133}I	20.8 h	529.9	87.0	3.06 ± 0.14	4.34 ± 0.14
^{135}I	6.57 h	1131.5	22.6	4.17 ± 0.25	5.49 ± 0.16
		1260.4	28.7	3.83 ± 0.42	
^{139}Ba	83.03 m	165.8	23.7	6.29 ± 0.42	7.49 ± 0.63
^{142}La	91.1 m	641.2	47.4	6.34 ± 0.24	7.01 ± 0.43
^{143}Ce	33.03 h	293.2	42.8	7.51 ± 0.35	6.95 ± 0.41

Table 3.3 Fission product yields in neutron-induced fission of ^{232}Th with average energy of 10.09 MeV

Nuclide	Half-life	Gamma-ray energy (keV)	Gamma Abundance (%)	Fission yield (%)	
				Present data	Literature [15]
^{77}Ge	11.3 h	416.3	21.8	3.15±0.16	
$^{85}\text{Kr}^{\text{m}}$	4.48 h	151.1	75.0	4.72±0.42	5.81± 0.20
^{87}Kr	76.3 m	402.5	50.0	5.31±0.39	7.44± 0.30
^{88}Kr	2.84 h	196.3	26.0	5.56±0.32	6.71± 0.25
$^{91}\text{Y}^{\text{m}}$	49.71 m	555.5	95.0	7.61±0.53	
^{91}Sr	9.63 h	749.8	23.3	6.60±0.28	7.15 ±0.20
		1024.0	33.0	7.43±0.56	
^{92}Sr	2.71 h	1384.9	90.0	6.62±0.64	6.62± 0.81
^{97}Zr	16.9 h	743.3	93.03	3.53±0.43	3.59 ±0.10
^{99}Mo	65.97 h	140.5	89.0	1.81±0.05	2.25± 0.23
^{132}Te	3.204 d	228.1	88.0	2.90±0.23	2.77± 0.09
^{133}I	20.8 h	529.9	87.0	3.27±0.31	4.32± 0.12
^{135}I	6.57 h	1131.5	22.6	4.45±0.26	5.58± 0.15
		1260.4	28.7	5.19±0.42	
^{139}Ba	83.03 m	165.8	23.7	5.71±0.32	6.61± 0.71
^{140}La	1.67 d	487.0	45.5	5.45±0.61	7.87± 0.35
^{142}La	91.1 m	641.2	47.4	5.54±0.29	6.84± 0.36
^{143}Ce	33.03 h	293.3	42.8	5.18±0.34	6.94± 0.33

The uncertainties associated to the measured cumulative yields come from the combination of two experimental data sets. The overall uncertainty is the quadratic sum of both statistical and systematic errors. The random error in the observed activity is particularly due to counting statistics, which is estimated to be 5-10 %. This can be accumulating the data for an optimum time period that depends on the half-life of the nuclide of interest. The systematic errors are due to uncertainties in neutron flux estimation (~4 %), irradiation time (~1%), detector efficiency (~5 %), the half-life of fission products and gamma-ray abundances (~2%). The overall uncertainty is found to range between 8-12%, coming from the combination of statistical error of 5-10% and a systematic error of 6 %.

The cumulative yields of different fission products of present work in the 10.09 MeV neutron-induced fission of ^{232}Th were determined for the first time. The literature data [15] at the mono-energetic neutron of 5.9 MeV and 7.6 MeV are given in the Table 1 and 2 to compare the present data at average neutron energy of 5.42 MeV and 7.76 MeV. There is no data available for mono-energetic neutron-induced fission of ^{232}Th at 10.09 MeV. Thus, the mono-energetic neutron induced fission yield data at 8.0 MeV from literature [15] are shown in Table 3 with the data of the 10.09 MeV from present work. It can be seen from Table 3.1-3.3 that the cumulative fission yields determined from the present work at three different flux weighted neutron energies are in general agreement with the literature data [15] based on mono-energetic neutron-induced fission of ^{232}Th . However, the fission yield data from the present work are for seven, fourteen and sixteen fission products for the neutron energy of 5.4 MeV, 7.75 MeV and 10.09 MeV, respectively. The yields of less number of fission products with decrease of neutron energy may be due to lower neutron flux and decrease of fission cross-section at lower neutron energy of 5.42 MeV. This may be also due the tailing in the neutron energy spectrum as shown in Fig.2. In spite of the tailing of neutron energy, the yields of number of fission products are as high as sixteen at higher neutron energy of 10.09 MeV. The yields of various fission products in the neutron energies of 5.42 MeV and 7.75 MeV from present work and comparable neutron energy from literature [15] are plotted in Fig. 3.3 and 3.4.

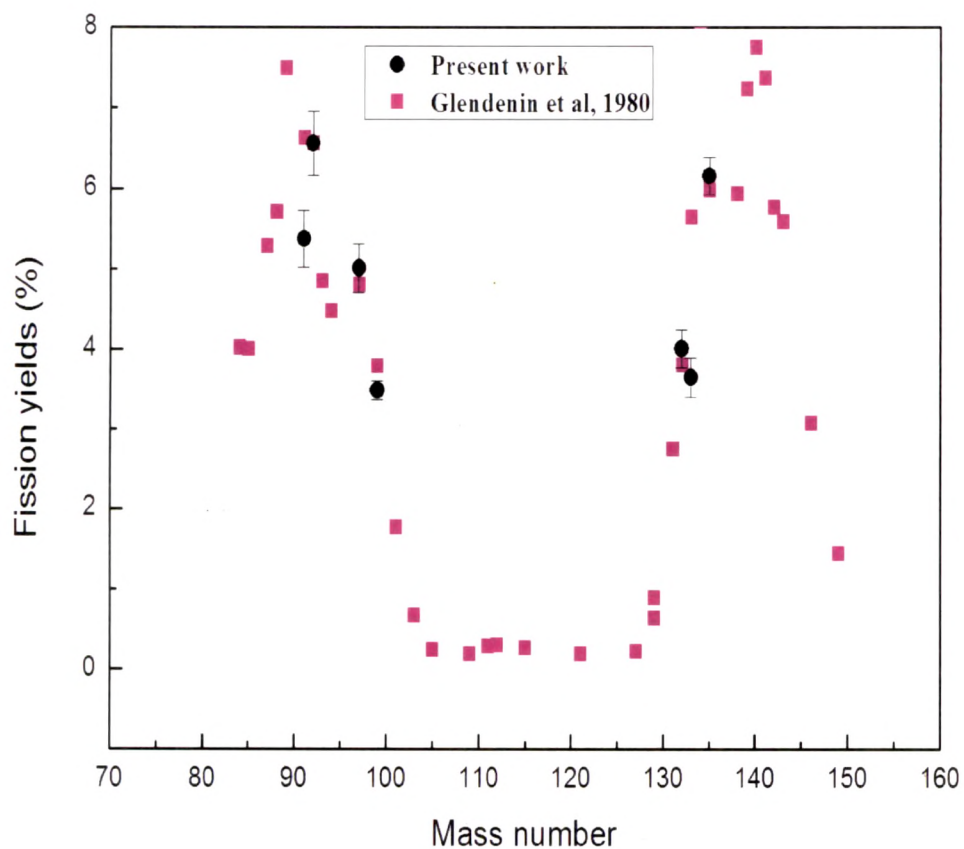


Fig. 3.3 Yields of fission products (%) as a function of mass number in the neutron-induced fission of ^{232}Th at average energy of 5.42 MeV along with the literature data

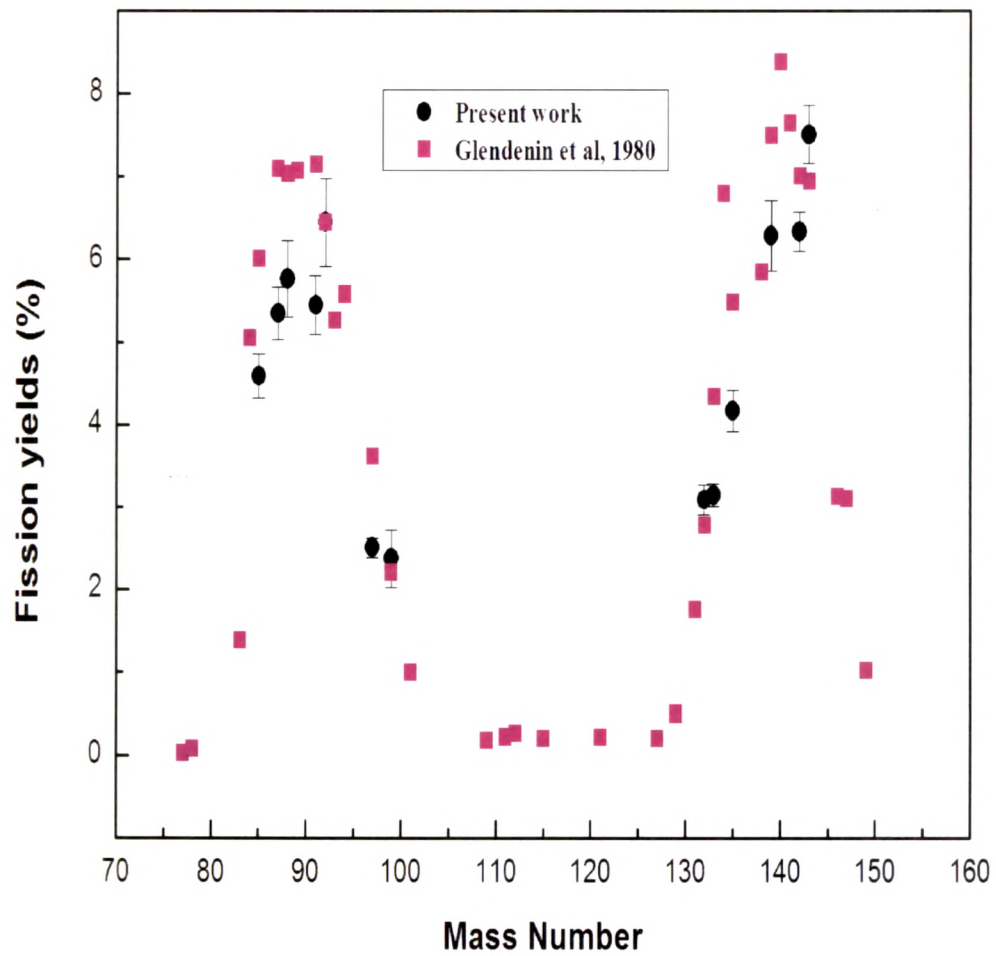


Fig. 3.4 Yields of fission products (%) as a function of mass number in the neutron-induced fission of ^{232}Th at average energy of 7.75 MeV along with the literature data

It can be seen from Fig. 3 and 4 that the higher yields of fission products around mass number of 134-135, 139-140 and 144-145 and their complementary products are clearly observed. In order to examine this aspect in better way, it is necessary to have more data around the above mentioned mass region.

3.6 Summary and Conclusions

The yields of various fission products in the neutron-induced fission of ^{232}Th have been determined using recoil catcher and off-line gamma-ray spectrometric technique with average energies of 5.42 MeV, 7.75 MeV and 10.09 MeV. The average neutrons were generated using the ^7Li (p, n) reaction at BARC-TIFR Pelletron, Mumbai, India. The fission products yields data in the 10.09 MeV neutron induced fission of ^{232}Th are determined for the first time. The present measured yields of the different fission products in the neutron-induced fission of ^{232}Th with average energies of 5.42 MeV and 7.75 MeV have been compared with the similar data of mono-energetic neutrons of comparable energy from literature and were found to be consistent. The effect of nuclear structure on fission products yields as a function of neutron energy has been examined. The following conclusions have drawn from this present work.

- In the present work, the yields of seven, fourteen and sixteen fission products in neutron induced fission of ^{232}Th at average neutron energy of 5.42 MeV, 7.75 MeV and 10.09 MeV were determined using recoil catcher and off-line gamma ray spectrometric technique. The yields of fission products at average neutron energy of 10.09 MeV were determined for the first time.
- The present data at average neutron energy of 5.42 MeV, 7.75 MeV and 10.09 MeV are in general agreement with the neutron induced fission data of ^{232}Th for mono-energetic neutron of 5.9 MeV, 7.6 MeV and 8.0 MeV, respectively.
- The yields of fission products around mass number 134 -135, 139 -140 and 144 - 145 and their complementary products are slightly higher than the yields of other fission products. This shows the effect of nuclear structure even at higher neutron energy.

References

- [1]. S. S. Kapoor, *Pramana J. Phys.* **59**, 941 (2002)
- [2]. F. Carminati et al, An Energy Amplifier for Cleaner and Inexhaustible Nuclear Energy
Production Driven by Particle Beam Accelerator, CERN Report No. CERN/AT/93-47 (ET)
1993
- [3]. C. Rubbia et al, Conceptual Design of a Fast Neutron Operated High Power Energy
Amplifier, CERN/AT/95-44 (ET) 1995
- [4]. C. D. Bowman, *Ann. Rev. Nucl. Part. Sci.* **48**, 505 (1998)
- [5]. S. Ganesan, *Pramana J. Phys.*, **68**, 257 (2007)
- [6]. H. N. Erten, A. Gruetter, E. Rossler, and H. R. Von Gunten, *Nucl. Sci. Eng.* **79**, 167 (1981).
- [7]. R. H. Iyer, C. K. Mathews, N. Ravindran, K. Rengan, D. V. Singh, M. V. Ramaniah, J.
Inorg. Nucl. Chem. **25**, 465 (1963)
- [8]. A. Turkevich and J. B. Niday, *Phys. Rev.* **84**, 52 (1951)
- [9]. K. M. Broom, *Phys. Rev.* **133**, 874 (1964)
- [10]. R. Ganapathy, P. K. Kuroda, *J. Inorg. Nucl. Chem.* **28**, 2071 (1966).
- [11]. Tin Mo, M. N. Rao, *J. Inorg. Nucl. Chem.* **30**, 345 (1968)
- [12]. L. H. Gevaert, R. E. Jervis, H. D. Sharma, *Can. J. Chem.* **48**, 641 (1970).
- [13]. L. Swindle, D. T. Moore, J. N. Beck, P. K. Kuroda, *J. Inorg. Nucl. Chem.* **33**, 3643 (1971)
- [14]. J. Trochon, H. A. Yehia, F. Brisard, and Y. Pranal, *Nucl. Phys. A* **318**, 63 (1979)
- [15]. L. E. Glendenin, J. E. Gindler, I. Ahmad, D. J. Henderson, and J. W. Meadows, *Phys. Rev.*
C 22, 152 (1980)

- [16]. S. T. Lam, L. L. Yu, H. W. Fielding, W. K. Dawson, and G. C. Neilson, Phys. Rev. C **28**, 1212 (1983).
- [17]. S. G. Mashnik et al, $^7\text{Li}(p,n)$ Nuclear data Library for Incident Proton Energies to 150 MeV, arXiv: nucl-th/0011066v117, Los Alamos National Laboratory (Nov.2000).
- [18]. J. F. Ziegler, M. D. Zeigler, J. P. Biersack, Nucl. Inst. Meth. B, **268**, 1818 (2010)
- [19]. C. H. Poppe et al, Phys. Rev. C **14**, 438 (1976).
- [20]. H. Naik et al, Eur. Phys. J. A. **47**, 51 (2011)
- [21]. P. M. Prajapati et al, Eur. Phys. J. A. **48**, 35 (2012)
- [22]. NuDat (BNL, U.S. A), www.nndc.bnl.gov/nudat2/